MOLECULAR AND CELLULAR BIOLOGY, July 2010, p. 3519–3530 Vol. 30, No. 14
0270-7306/10/$12.00 doi:10.1128/MCB.00394-10

Ric-8A and Giα Recruit LGN, NuMA, and Dynein to the Cell Cortex To Help Orient the Mitotic Spindle▽‡

Geoffrey E. Woodard,[1]† Ning-Na Huang,[1]† Hyeseon Cho,[1] Toru Miki,[2] Gregory G. Tall,[3] and John H. Kehrl[1]*

B-Cell Molecular Immunology Section, Laboratory of Immunoregulation, National Institute of Allergy and Infectious Disease, Bethesda, Maryland 20892-1888[1]; Laboratory of Cellular Signaling, Department of BioEngineering, Nagaoka University of Technology, 1603-1 Kamitomioka, Nagaoka, Niigata 940-2188, Japan[2]; and Department of Pharmacology and Physiology, University of Rochester Medical Center, Rochester, New York 14642[3]

Received 6 April 2010/Accepted 4 May 2010

In model organisms, resistance to inhibitors of cholinesterase 8 (Ric-8), a G protein α (Gα) subunit guanine nucleotide exchange factor (GEF), functions to orient mitotic spindles during asymmetric cell divisions; however, whether Ric-8A has any role in mammalian cell division is unknown. We show here that Ric-8A and $G\alpha_i$ function to orient the metaphase mitotic spindle of mammalian adherent cells. During mitosis, Ric-8A localized at the cell cortex, spindle poles, centromeres, central spindle, and midbody. Pertussis toxin proved to be a useful tool in these studies since it blocked the binding of Ric-8A to $G\alpha_i$, thus preventing its GEF activity for $G\alpha_i$. Linking Ric-8A signaling to mammalian cell division, treatment of cells with pertussis toxin, reduction of Ric-8A expression, or decreased $G\alpha_i$ expression similarly affected metaphase cells. Each treatment impaired the localization of LGN (GSPM2), NuMA (microtubule binding nuclear mitotic apparatus protein), and dynein at the metaphase cell cortex and disturbed integrin-dependent mitotic spindle orientation. Live cell imaging of HeLa cells expressing green fluorescent protein-tubulin also revealed that reduced Ric-8A expression prolonged mitosis, caused occasional mitotic arrest, and decreased mitotic spindle movements. These data indicate that Ric-8A signaling leads to assembly of a cortical signaling complex that functions to orient the mitotic spindle.

The cortical capture of astral microtubules is essential to generate the forces needed for mitotic spindle positioning for both symmetric and asymmetric cell divisions (23, 29). Failure to either capture astral microtubules or the inappropriate application of pulling forces adversely affects mitotic spindle orientation, and can impede embryogenesis and alter cell fate decisions. Studies examining mitotic spindle orientation in *Drosophila* embryonic and larval neuroblasts have identified two critical pathways, the Gα/Pins/Mud pathway and the Pins/Dlg/Khc73 pathway (29). The heterotrimeric G-protein α subunit (Gα), Pins (Partner-of-Inscuteable), and Mud (Mushroom body defect) are members of an evolutionarily conserved noncanonical G-protein signaling pathway, which form a tripartite protein complex linked to the apical Par complex by the adapter protein Inscuteable (29, 37). Reducing the level of $G\alpha_i$, Pins, or Mud prevents neuroblast mitotic spindle alignment. A second spindle orientation pathway involves Pins, the tumor suppressor Discs large (Dlg) and the microtubule plus-end-directed kinesin heavy chain 73 (Khc73). Khc73 binds Dlg and coimmunoprecipitates with Pins. Khc73 localized to astral microtubules can induce Pins-Dlg cortical polarity (27).

In canonical G-protein signaling pathways, the binding of ligand to a seven-transmembrane receptor triggers a heterotrimeric G-protein α subunit (Gα) to exchange GTP for GDP, resulting in the dissociation of the Gα subunit from its associated Gβγ heterodimer (12, 20). This exposes interactive sites in the Gα and Gβγ subunits, allowing their binding to and activation of downstream effectors. Since Gα subunits possess an intrinsic GTPase activity, GTP hydrolysis leads to the reassembly of heterotrimeric G protein causing signaling to cease. In noncanonical G-protein signaling the seven-transmembrane receptor is replaced by an intracellular guanine nucleotide exchange factor, such as Ric-8 (37). In studies in *Drosophila* and *Caenorhabditis elegans* Ric-8 has been shown to positively regulate $G\alpha_i$ activity and is essential for asymmetric cell divisions (1, 2, 5, 8, 11, 36). Although initially characterized as a guanine nucleotide exchange factor (GEF) for isolated $G_\alpha$subunits, more recent biochemical studies have shown that Ric-8A (the mammalian equivalent of Ric-8) also acts on a complex of GDP-$G\alpha_i$, the mammalian Pins homolog LGN, and NuMA (nuclear mitotic apparatus protein; the mammalian equivalent of Mud) catalytically releasing GTP-$G\alpha_i$ and causing liberation of NuMA from LGN (30, 31). Ric-8A can also catalyze guanine nucleotide exchange on $G\alpha_{i1}$ bound to the GPR/GoLoco exchange inhibitor AGS3, a paralog of LGN (33). During mitosis the N-terminal portion of LGN binds NuMA and the C-terminal domain binds GDP-$G\alpha_i$ and the trimolecular complex localizes to the cell cortex, where the dynamic release of NuMA from LGN may regulate aster microtubule pulling during cell division (3, 9, 10, 22).

In the present study we examined the role of Ric-8A in

* Corresponding author. Mailing address: B-Cell Molecular Immunology Section, Laboratory of Immunoregulation, National Institute of Allergy and Infectious Disease, 10 Center Drive, MSC 1888, Bethesda, MD 20892-1752. Phone: (301) 496-3819. Fax: (301) 402-0070. E-mail: jkehrl@niaid.nih.gov.

† G.E.W. and N.-N.H. contributed equally to this study.

‡ Supplemental material for this article may be found at http://mcb.asm.org/.

▽ Published ahead of print on 17 May 2010.

mitotic spindle orientation in adherent cells and in polarized MDCK cells. In nonpolarized adherent cells cell such as HeLa, integrin mediated cell-substrate adhesion orients the mitotic spindle parallel to the substratum, and thereby both daughter cells remain attached. This requires the actin cytoskeleton, astral microtubules, the microtubule plus end tracking protein EB1, myosin X, cdc42, LIM kinase 1, and phosphatidylinositol(3,4,5)-triphosphate (PIP_3) (13, 18, 32, 34, 35). PIP_3 may direct dynein/dynactin-dependent pulling forces on the spindle midcortex to orient the mitotic spindle (34). In polarized cells such as Madin-Darby canine kidney (MDCK) cells, the mitotic spindle is constrained by the topology of the cell and cortical cues provided by adherens junctions (24). In contrast to HeLa cells these cues are insensitive to phosphatidylinositol 3-kinase (PI3K) inhibition, which blocks the generation of PIP_3 (34). We found that inhibiting either Ric-8A or $G\alpha_i$ expression impairs the orientation of the metaphase mitotic spindle in HeLa cells and pertussis toxin, which blocks Ric-8A triggered nucleotide exchange, disrupts the normal mitotic spindle alignment of both HeLa and MDCK cells. Impairment of Ric-8A expression or function inhibits the localization of $G\alpha_{i1}$, LGN, NuMA, and dynein to the metaphase cortex opposite the spindle poles.

MATERIALS AND METHODS

Cells. HeLa and MDCK cells were purchased (American Tissue Culture Collection) and maintained as suggested. HeLa α-tubulin green fluorescent protein (GFP) cells were created by permanently transfecting HeLa cells with a construct that expresses α-tubulin fused to GFP, along with the selection marker neomycin. HeLa cells permanently expressing α-tubulin-GFP were selected with G418 (Calbiochem). MDCK Cells were plated at subconfluent densities onto glass coverslips. In some instances, HeLa cells were synchronized by double thymidine block and then arrested in metaphase by a 30-min treatment with the proteasome inhibitor MG132 as described previously (34).

Effect of pertussis toxin on Ric-8A GEF activity. Myristoylated $G\alpha_i$ (400 nM) was ADP-ribosylated using 4 μg of pertussis toxin protomer (List Biological Laboratories)/ml in the presence of 40 nM Gβ1γ2, 100 mM Tris (pH 7.7), 6 mM $MgCl_2$, 2 mM EDTA, 4 μM dithiothreitol, 40 μM NAD, and 1 μM GDP for 1 h at 25°C. A parallel reaction was spiked with ^{32}P-labeled α-NAD (3,000 cpm/pmol). The labeled $G\alpha_i$ from this reaction was filter bound, washed, and subjected to liquid scintillation counting to determine the stoichiometry of ADP-ribosylation. ADP-ribosylated or mock-treated $G\alpha_i$ (200 nM) was then incubated with or without Ric-8A (200 nM) in GTPγS binding reactions containing 20 mM HEPES (pH 8.0), 100 mM NaCl, 2 μM dithiothreitol, 1 mM EDTA, 10 mM $MgCl_2$, and 0.05% lubrol $C_{12}E_{10}$. Duplicate aliquots were withdrawn at the specified times, quenched, and bound to filters. The filters were washed and subjected to liquid scintillation counting to determine the stoichiometry of $G\alpha_i$ GTPγS binding.

Reagents and antibodies. Hoechst 33342 (Invitrogen) was used at a concentration of 100 ng/ml, pertussis toxin (Calbiochem) was used at 400 ng/ml for 4 h, Taxol (Sigma) was used at 200 nM for 2 h, and nocodazole (Sigma) used at 200 nM for 2 h. The primary antibodies used for Western blotting were as follows: anti-Erk mouse monoclonal antibody (1:1,000 dilution [Santa Cruz]) and anti-Ric-8A rabbit polyclonal antibody (1:10,000 [G. Tall]). The secondary antibodies used for Western blotting were a polyclonal anti-mouse immunoglobulin conjugated to horseradish peroxidase and a polyclonal anti-rabbit immunoglobulin similarly conjugated. Primary antibodies used for immunofluorescence were as follows: anti-Ric-8A rabbit polyclonal antibody (1:2,000 [G. Tall]), anti-CENP-E mouse monoclonal antibody (1:100 [Abcam]), anti-β-tubulin mouse monoclonal directly fluorescein isothiocyanate (FITC)-labeled antibody (1:25 [Abcam]), anti-β tubulin rabbit polyclonal antibody (1:200 [Abcam]), anti-Aurora B mouse monoclonal antibody (1:200 [Abcam]), anti-LGN antibody (1:100 [J. Blumer, University of South Carolina]), anti-NuMA mouse monoclonal antibody (1:100 [EMD Biosciences]), anti-NuMA rabbit polyclonal antibody (1:100 [D. Compton, Dartmouth College]), anti-$G\alpha_{i1}$ antibody (1:25 [Santa Cruz]), anti-$G\alpha_{i2}$ antibody (1:100 [EMD Biosciences]), anti-$G\alpha_{i3}$ antibody (1:100 [EMD Biosciences]), and anti-γ-tubulin antibody (1:1,000 [Sigma]). The secondary antibodies used for immunofluorescence were as follows: polyclonal anti-mouse immunoglobulin Alexa 488- or Alexa 568-conjugated antibody (1:1,000 [Invitrogen]), polyclonal anti-rabbit immunoglobulin Alexa 488- or Alexa 568-conjugated antibody (1:1,000 [Invitrogen]), and polyclonal anti-goat immunoglobulin Alexa 488- or Alexa 568-conjugated antibody (1:1,000 [Invitrogen]).

Plasmids, shRNAs, and siRNAs. GFP fusion constructs of human Ric-8A were made using pcDNA3.1/NT-GFP and pcDNA6.2/N-EmGFP-GW Ric-8A. A human pSM2 retroviral shRNAmir construct (Open Biosystems) targeting Ric-8 mRNA was screened for efficacy by immunoblotting Ric-8 levels in transiently transfected HeLa cells. The hairpin sequence is 5′-TGCTGTTGACAGTGAG CGAGGAGTTCATGGGAGTGAATATTAGTGAAGCCACAGATGTAAT ATTCACTCCCATGAACTCCGTGCCTACTGCCTCGGA-3′, which targets the sequence from nucleotides (nt) 1226 to 1244 (GenBank NM_021932.4) in the Ric-8A mRNA. The screening transfections, as well as those subsequently performed, were done with HeLa cells using Lipofectamine 2000 according to the manufacturer's protocol (Invitrogen). In all experiments, a second transfections was performed 2 days after the primary transfection. The transfected cells were analyzed 2 days after the second transfection. A parallel transfection with a nonsilencing pSM2 shRNAmir retroviral shRNA from the same manufacturer was performed for each experiment. Both the $G\alpha_i$ and Ric-8A small interfering RNA (siRNA) knockdowns were performed in HeLa cells by following a previously described protocol (14). $G\alpha_{i1/3}$ (nt 721 to 739; 5′-CCGAAUGCAUGAA AGCAUG-3′) and $G\alpha_{i2}$ (nt 681 to 699; 5′-CUUGAGCGCCUAUGAC UUG-3′) siRNAs and control siRNAs were purchased from Dharmacon. For Ric-8A siRNA silencing, an ON-TARGET plus SMARTpool L-016121-01-0005 was used (sequences 5′-GGGGAGAUGCUGCGGAACAUU-3′, 5′-AGAACUUU CCAUACGAGUAUU-3′, 5′-CAGGAUGCCAUGUGCGAGAUU-3′, and 5′-CAGAGGAGUUCCACGGCCAUU-3′ based on GenBank accession number NM_021932.4). The si*CONTROL* Non-Targeting siRNA Pool #1 was used for control siRNA transfections (Dharmacon).

Western blots. A total of 10×10^6 cells were lysed with 0.5 ml of radioimmunoprecipitation assay lysis buffer (50 mM Tris-HCl [pH 7.4], 150 mM NaCl, 1% NP-40, 0.5% sodium deoxycholate, 0.1% sodium dodecyl sulfate [SDS]) with a protease inhibitor cocktail. The detergent-insoluble materials were removed, and equal amounts of protein were fractionated by 10 to 20% Tricine SDS-PAGE and transferred to nitrocellulose membranes. Membranes were blocked with 5% milk in phosphate-buffered saline (PBS) for 1 h and then incubated with an appropriate dilution of the primary antibody in 5% milk in PBS overnight. The blots washed and then incubated with secondary antibody for 2 h. The signal was detected by enhanced chemiluminescence (Amersham).

Immunocytochemistry. Cells were fixed either in 3.7% paraformaldehyde, diluted from a 37% stock solution in PBS for 20 min at room temperature, or in cold (−20°C) methanol. Paraformaldehyde-fixed cells were permeabilized by 0.5% Triton X-100 in PBS for 20 min at room temperature. The appropriate dilution of primary added, which was diluted in PBS with 2% serum from the species that the secondary antibody was made, followed by incubation from 2 h to overnight. The slides were washed three times in PBS prior to the addition of the secondary antibody for 0.5 h. Three PBS washes were done prior to imaging. DNA was stained with DRAQ5 (Biostatus, Ltd.) according to the manufacturer's recommendations. For Dynein and $p150^{glue}$ staining HeLa cells were pre-extracted in 0.5% Triton X-100 in PHEM buffer (60 mM PIPES, 25 mM HEPES, 10 mM EGTA, 4 mM $MgSO_4$) with 5 μM Taxol for 1 min, and fixed in methanol at −20°C for 5 min. For phalloidin and $G\alpha_i$ staining, HeLa cells were paraformaldehyde fixed and permeabilized as described above. Cells were then stained with primary Gα antibodies overnight, washed with PBS, and stained with secondary antibodies plus Alexa Fluor 488-phalloidin for 2 h.

Cell imaging and image analysis. All fluorescent images were collected on inverted confocal microscopes. A Perkin-Elmer Ultraview spinning wheel confocal system mounted on a Zeiss Axiovert 200 and equipped with an argon-krypton laser, an Orca-ERII charge-coupled device camera (Hamamatsu), and filters suitable for the visualization of both FITC, and red dyes were used for imaging the fixed samples and for short-term live cell imaging. Single images or z-stacks of 5 to 30 images were collected using a ×63 1.4-numerical-aperture (NA) or a ×100 1.45-NA oil objective lens. For live cell imaging, images were acquired every 30 s for 10 to 20 min using 50% laser power and 100 millisecond exposures. A SP5 confocal microscope (Leica Microsystems) with a ×40 1.25-NA objective lens was used for the long-term live cell imaging. Excitation was with an argon laser at 488 nm, with laser power at 2%. Four slice separated by 3 μm were taken every 3 min for the duration of the imaging (8 to 12 h). The incubation chamber was a Pe-Con incubator S with heating insert P, set to 37°C with 5% CO_2. Adobe Photoshop CS was used to prepare composite images and for annotations. Imaris 6.0.0 (Bitplane AG), Ultraview 5.5 (Perkin-Elmer), Adobe Photoshop CS (Adobe systems), and IP Lab 4.04 (Scanalytics) were used for the

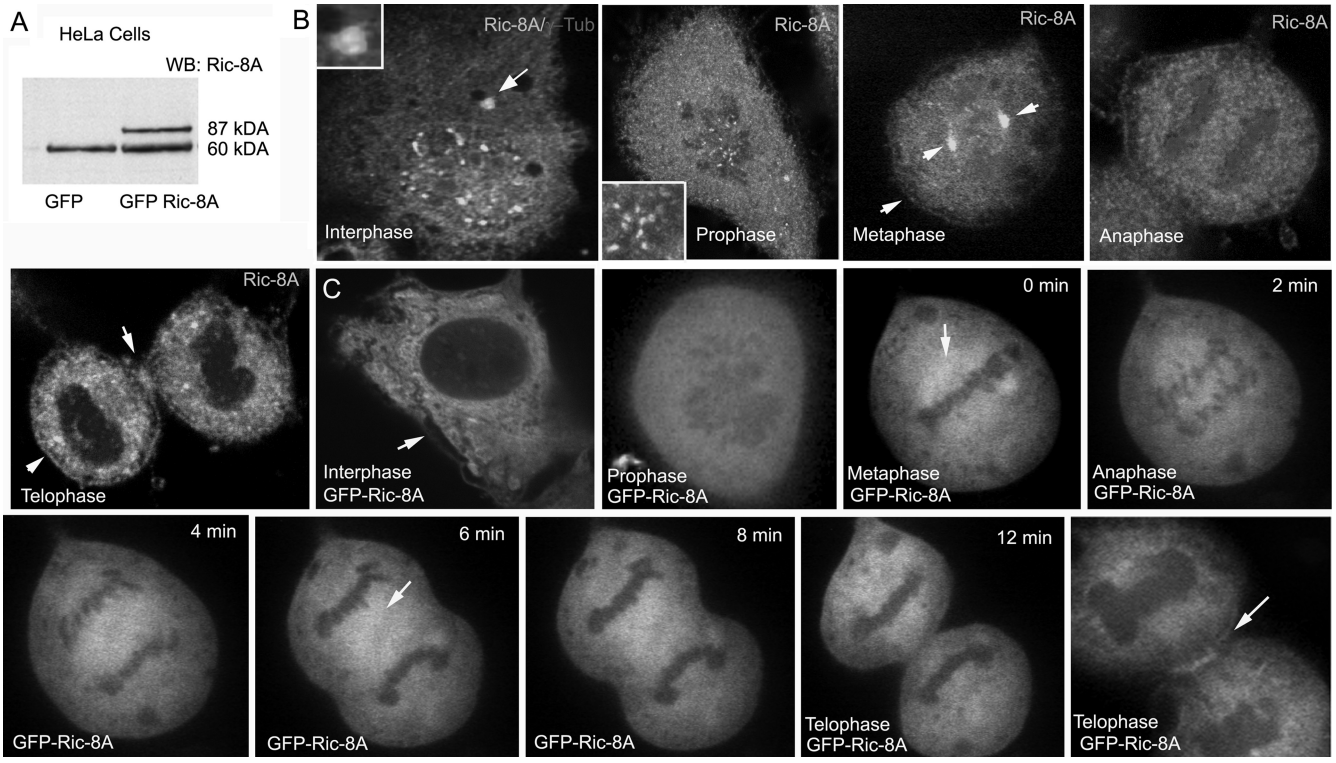

FIG. 1. Localization of Ric-8A in HeLa cells during the cell cycle. (A) Immunoblot of Ric-8A expression. HeLa cell lysates from cells transfected with GFP or GFP-Ric-8A were immunoblotted with a Ric-8A antibody. Endogenous Ric-8A and GFP-Ric-8A had estimated molecular masses of 60 and 87 kDa, respectively. (B) Confocal images of HeLa Cells immunostained as indicated. Ric-8A and γ-tubulin colocalize (arrow in first panel) in the centrosomes of interphase cells (the inset shows a ×4 electronic zoom). The second panel shows Ric-8A immunostaining in prophase cells in a pattern consistent with centromere staining (the inset is a ×4 electronic zoom of region overlapping condensing chromosomes). Centrosome staining (third panel) is indicated by arrows. Midbody region staining and cell cortex in a telophase cell is shown with arrows (the last panel). (C) Localization of GFP-Ric-8A. HeLa cells were transfected with GFP-Ric-8A, and live cell images were acquired 2 days after transfection. The interphase cell and prophase cell are different cells. The localization at the cell cortex in interphase cell indicated by an arrow. Several images from a time series are shown beginning with time zero (metaphase) to 12 min later, early telophase. The last panel is from another cell imaged at telophase (×1.5 electronically zoomed). Arrows point to areas of enhanced expression.

image processing. The collected images from the time-lapse imaging were processed using Imaris and reconstructed into QuickTime movies. All movies from long-term live cell imaging are shown at a frame rate of 10/s, while the short-term live cell imaging is shown at a frame rate of 5/s. The polygon function in Imaris was used to determine the mitotic spindle orientation in sequential time-lapse images. The duration of mitosis was measured from when the mitotic spindle was first visualized until the spindle poles were observed to separate. The spindle angle was measured as described previously (34). Z-stack images (0.5 μm apart) of metaphase cells stained with anti-γ-tubulin, anti-α-tubulin antibodies and for DNA were obtained, and the linear and the vertical distances between the two poles of a metaphase spindle were measured. The spindle angle was calculated by inverse trigonometric function.

RESULTS

Localization of Ric-8A in interphase and mitotic cells. Since little information is available on the intracellular localization of mammalian Ric-8A, we examined it during phases of the cell cycle using human HeLa cells and a Ric-8A antibody or by monitoring the localization of a GFP fused to Ric-8A (GFP-Ric-8A). The Ric-8A antibody was raised against recombinant protein in rabbits and recognizes endogenous and transfected Ric-8A (Fig. 1A). In addition, reducing Ric-8A expression markedly reduced the amount of Ric-8A immunostaining that we observed (see below). We noted that the Ric-8A antibody stained the cytosol, centrosomes as it colocalized with the centrosome marker γ-tubulin, and dotlike structures in the nuclei of interphase cells (Fig. 1B). In prophase and metaphase we detected Ric-8A immunoreactivity at the spindle poles, along the cell cortex, in the cytosol, and in a centromerelike pattern on chromosomes (Fig. 1B). To verify its presence in the centromere, we colocalized the Ric-8A immunostaining with a known centromere marker, the centromere-associated protein E (CENP-E; see Movie S1 in the supplemental material). $G\alpha_i$ has also been reported to localize in the centromere region (6). When the cells progressed to anaphase/telophase, the distribution of Ric-8A immunostaining did not change significantly, although an enrichment of Ric-8A in the midbody region was noted (Fig. 1B). Next, we expressed a GFP-Ric-8A fusion protein and examined its localization during phases of the cell cycle. All attempts to permanently express GFP-Ric-8A in HeLa cells or the human T-cell leukemia cell line Jurkat failed, so we relied on transient transfections. The transient transfection of GFP-Ric-8A into HeLa reduced the number of mitotic cells observed, and only cells expressing low levels of the GFP-Ric-8A fusion protein progressed through the cell cycle. In interphase cells, the GFP fusion protein showed a distribution

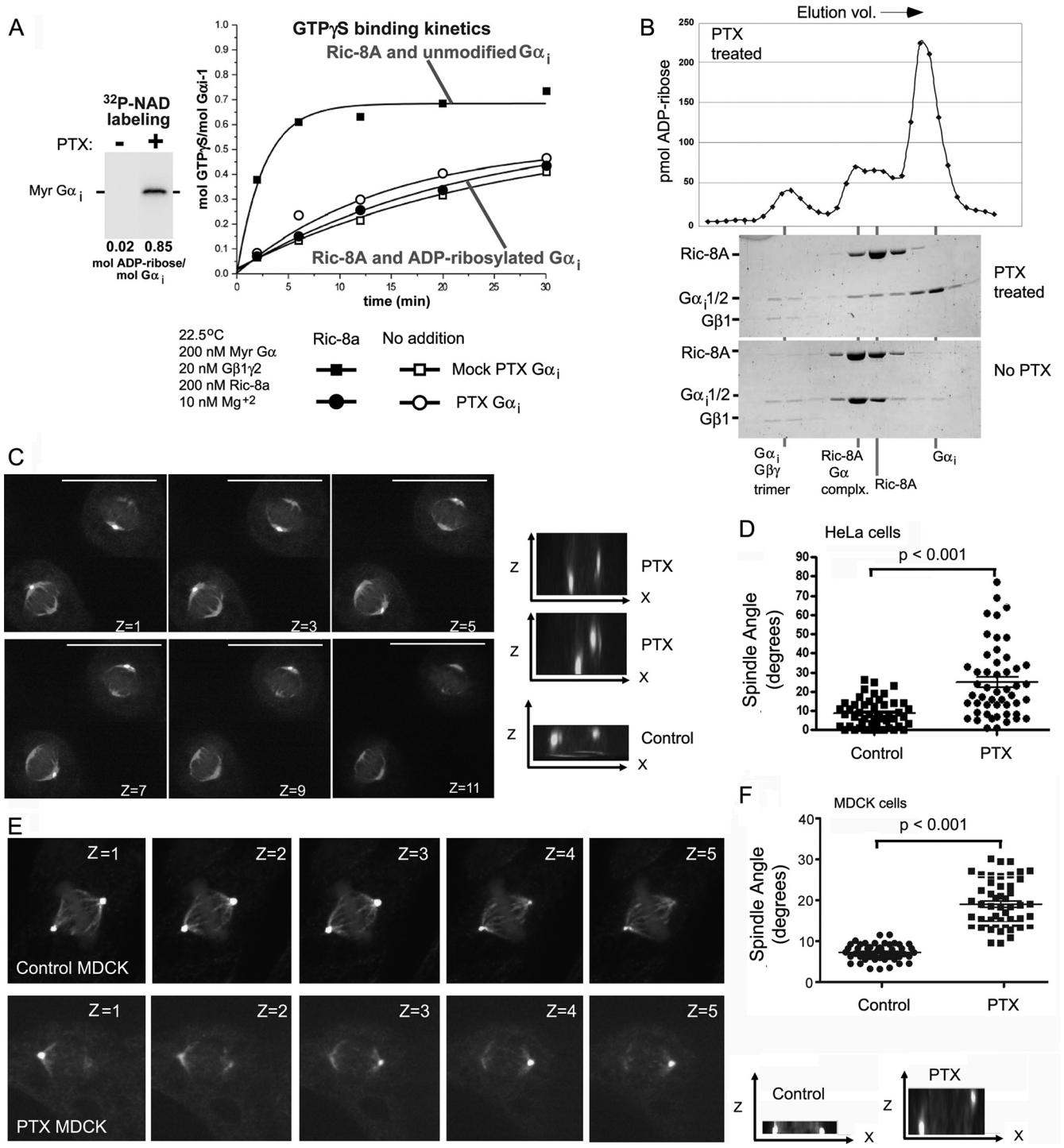

FIG. 2. Effect of pertussis toxin on Ric-8 catalytic activity and mitotic spindle orientation. (A) Ric-8A does not activate ADP-ribosylated $G\alpha_i$. Myristoylated $G\alpha_i$ was ADP-ribosylated using NAD and pertussis toxin (inset). The kinetics of GTPγS binding to ADP-ribosylated (circles) and mock-treated (squares) $G\alpha_i$ were determined in the presence (solid symbols) or absence (open symbols) of Ric-8A. (B) Ric-8A does not appreciably bind ADP-ribosylated $G\alpha_i$. ADP-ribosylated or mock treated $G\alpha_i$ was mixed with purified Ric-8A and resolved by gel filtration. The gel filtration eluates were fractionated, and the fractions were analyzed by Coomassie blue-stained SDS-PAGE for protein content. The positions where each species eluted from the columns are denoted below these gels. Ric-8A formed a stoichiometric complex with unmodified $G\alpha_i$ (no pertussis toxin) and virtually no complex with ADP-ribosylated $G\alpha_i$ (pertussis toxin [PTX] treated). The elution profile of ADP-ribose labeling in the pertussis toxin treated reaction is shown above the gel. (C and D) Disoriented mitotic spindle in pertussis toxin-treated HeLa cells. HeLa cells were treated with pertussis toxin (400 ng/ml for 4 h) prior to fixation and immunostaining for β- and γ-tubulin. Shown are selected confocal z-stacks at 0.5-μm intervals (top). *x-z* projections of the images of cells treated with pertussis toxin or not (cont) are also shown (right). The spindle angle (α°) was measured in metaphase cells. The distribution and averages (bar; means ± the standard deviations [SD]; $n = 50$) of spindle angles from control and pertussis toxin-treated cells are indicated. The *P* value was <0.001 compared to control cells as determined by the

similar to that of endogenous Ric-8A except that the strong nuclear localization noted with the Ric-8A antibody was not observed (Fig. 1C). As with many centrosomal proteins the GFP-Ric-8A fusion protein was only observed intermittently in centrosomes. During the phases of the cell cycle the GFP-Ric-8A fusion protein localized throughout the cytosol, although it showed some enrichment at the cell cortex and in the mitotic spindle (Fig. 1C; see Movie S2 in the supplemental material). The prominent centromere localization noted with the Ric-8A antibody was not seen with the GFP fusion protein, although we noted weak GFP expression overlying the condensing chromosomes. We also noted the GFP fusion protein in the midbody and along the adjacent cell cortex at telophase (Fig. 1C, last panel). We repeated these experiments with GFP fused to the C terminus of Ric-8A and found that both constructs gave similar patterns of expression (data not shown). Previously, Ric-8A was identified as coprecipitating protein using a phosphorylation-specific antibody termed P190 that reacts with several members of the chromosomal passenger complex (CPC [38]). CPC proteins are known to regulate chromosomal segregation and cytokinesis (25). Similar to what was reported, we found that immunostaining with the P190 antibody gave a pattern of reactivity similar to that we observed using with our Ric-8A antibody, although it showed a higher level of reactivity in the spindle region (data not shown).

Pertussis toxin inhibits Ric-8A triggered nucleotide exchange by blocking the binding of Ric-8A to $G\alpha_i$. While used extensively to inhibit signaling through Gi-linked receptors, the effect of pertussis toxin on Ric-8A triggered $G\alpha_i$ nucleotide exchange was unknown. To test its effect, we treated myristoylated $G\alpha_i$ with pertussis toxin and NAD in the presence of substoichiometric $G\beta\gamma$. A total of 85% of the $G\alpha_i$ was ADP-ribosylated by this treatment (Fig. 2A). ADP-ribosylated or mock-treated $G\alpha_i$ was then incubated with Ric-8A and GTPγS to assess the kinetics of Ric-8A-stimulated GTPγS binding. Ric-8A stimulated the intrinsic exchange rate of unmodified, but not ADP-ribosylated $G\alpha_i$ (Fig. 2A). The intrinsic exchange rates of modified and unmodified $G\alpha_i$ remained the same. Next, we examined whether $G\alpha_i$-ADP-ribosylation abrogated the binding of Ric-8A to $G\alpha_i$ (Fig. 2B). We incubated purified Ric-8A with unmodified or pertussis toxin treated $G\alpha_i$ in the presence of GDP, ran the reactions over sizing columns to resolve the Ric-8A:$G\alpha_i$ complex from individual monomers, and analyzed the fractions by Coomassie blue-stained gel and scintillation counting to quantify the amount of ADP-ribose label. Unmodified $G\alpha_i$ formed a 1:1 stoichiometric complex with Ric-8A of ~100 kDa, whereas the majority of ADP-ribosylated $G\alpha_i$ did not bind Ric-8A and eluted as a labeled monomer (~40 kDa). The substoichiometric $G\beta\gamma$ component of each reaction bound an equal amount of $G\alpha_i$ (modified or unmodified) and eluted as heterotrimer with an aberrantly high apparent molecular mass (~300 kDa).

Pertussis toxin treatment interferes with the normal alignment of the metaphase mitotic spindle in HeLa and MDCK cells. Since the ADP-ribosylation of $G\alpha_i$ subunits prevented the initial interaction between Ric-8A and $G\alpha_i$-GDP, pertussis toxin could be used to examine the role of $G\alpha_i$ nucleotide exchange in mitotic spindle orientation. We treated exponentially growing or synchronized HeLa cells plated on collagen coated plates with pertussis toxin for 4 h or not. The cells were fixed, immunostained for β-tubulin and γ-tubulin, and stained with a DNA labeling dye. The orientation of mitotic spindle of metaphase cells in relation to the substratum was determined. As reported previously, the majority of the control cells aligned their mitotic spindle parallel to the substratum (35); however, many of the pertussis toxin treated cells failed to do so (Fig. 2C). Images of confocal z-stacks acquired at 0.5-μm intervals of pertussis toxin-treated metaphase cells showed the spindle poles were not aligned to the substratum. The *x-z* projections of the γ-tubulin staining from two pertussis toxin-treated cells and one control cell shows the nonparallel alignment of the mitotic spindles of the pertussis toxin treated cells (Fig. 2C). The average angle of the mitotic spindle from 50 control metaphase cells was 8.4° (standard deviation [SD] = 7.2) and that from 50 pertussis toxin-treated metaphase cells was 24.8° (SD = 18.9) (Fig. 2D). In contrast to using cortical signals emanating from the substratelike HeLa cells, polarized MDCK cells orient their mitotic spindle by using cortical cues provided by adherens junctions (24). Although these cues are insensitive to PI3K inhibition (19), they were disrupted by pertussis toxin treatment. Images of confocal z-stacks acquired at 0.5-μm intervals and the *x-z* projection of a pertussis toxin-treated metaphase cells showed the misalignment of the spindle poles (Fig. 2E). Measuring the average angle of the mitotic spindle from 50 control metaphase MDCK cells (7.3°; SD = 2) and 50 pertussis toxin-treated MDCK cells (19.2°; SD = 5.6) confirmed the difference (Fig. 2F).

Interference with Ric-8A or $G\alpha_i$ expression inhibits alignment of the metaphase mitotic spindle in HeLa cells. If the predominant effect of pertussis toxin was to inhibit Ric-8A triggered $G\alpha_i$ nucleotide exchange, a reduction in Ric-8A or $G\alpha_i$ expression should produce the same phenotype. To examine that possibility, we used a Ric-8A shRNA or a pool of Ric-8A siRNAs to knock down its expression and a pool of siRNAs that targets $G\alpha_{i1}$, $G\alpha_{i2}$, and $G\alpha_{i3}$ expression in HeLa cells (14). Both the siRNA pools and the shRNA reduced the expression of their targets (Fig. 3A and B). The Ric-8A knockdown did not affect $G\alpha_i$ expression at the cell cortex of interphase cells (data not shown). Knockdown, wortmannin-treated, and control cells were immunostained for β- and γ-tubulin, and the orientations of metaphase mitotic spindles

Mann-Whitney test. (E and F) Disoriented mitotic spindle in pertussis toxin-treated MDCK cells. MDCK cells were grown to confluence on glass dishes for more than 90 h to allow the cells to become polarized prior to their treatment with pertussis toxin (400 ng/ml for 4 h). Afterward, the cells were fixed and immunostained for β- or γ-tubulin. Shown are selected confocal images from a 0.5-μm image stack (top). *x-z* projections of the images of untreated or (control) pertussis toxin-treated cells are also shown (lower right). The spindle angle (α°) was measured in metaphase cells. The distribution and averages (bar; means ± the SD; $n = 50$) of spindle angles from control and pertussis toxin-treated cells are indicated. The P value was <0.001 compared to control cells as determined by the Mann-Whitney test.

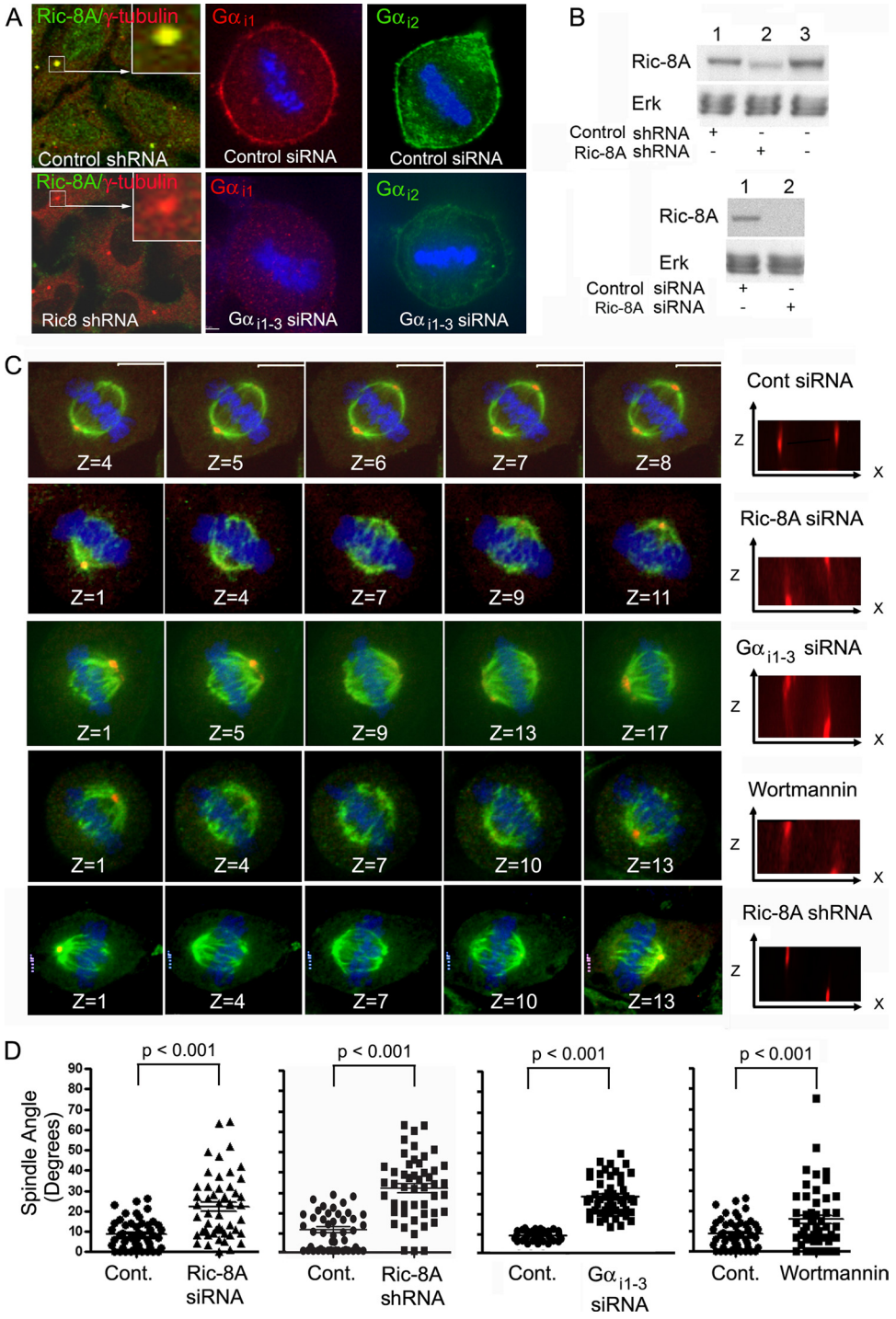

FIG. 3. $G\alpha_i$ and Ric-8A knockdowns impair integrin-mediated metaphase spindle orientation. (A) Confocal images of Ric-8A and $G\alpha_{i1-3}$ knockdown or control cells immunostained as indicated. DNA is blue. (B) Western blot of HeLa cells expressing either the Ric-8A shRNA or the Ric-8A siRNAs versus controls. Equal loading was verified by the p42/44 MAPK (Erk) levels. (C) Disoriented spindles in knockdown or wortmannin-treated cells. HeLa cells were doubly transfected with Ric-8A, $G\alpha_{i1-3}$, or control siRNAs, treated with wortmannin (10 nM) for 2 h, or double transfected with the Ric-8A shRNA or a control shRNA (results not shown) prior to fixation and immunostaining for β-tubulin (green) or γ-tubulin (red). DNA is blue. Shown are selected confocal images from a z-stack (0.5 μm between slices). *x-z* projections of the spindles are shown to the right. The spindle angle (α°) was measured in metaphase cells. (D) Distribution and averages (bar; means ± the SD; $n = 50$) of spindle angles from the appropriate control cells or treated cells: control (Cont.) versus Ric-8A siRNA, control versus Ric-8A shRNA, control versus $G\alpha_{i1-3}$ siRNA, and control versus wortmannin. Each of the treated populations was significantly different from control cells ($P < 0.001$) as determined by the Mann-Whitney test.

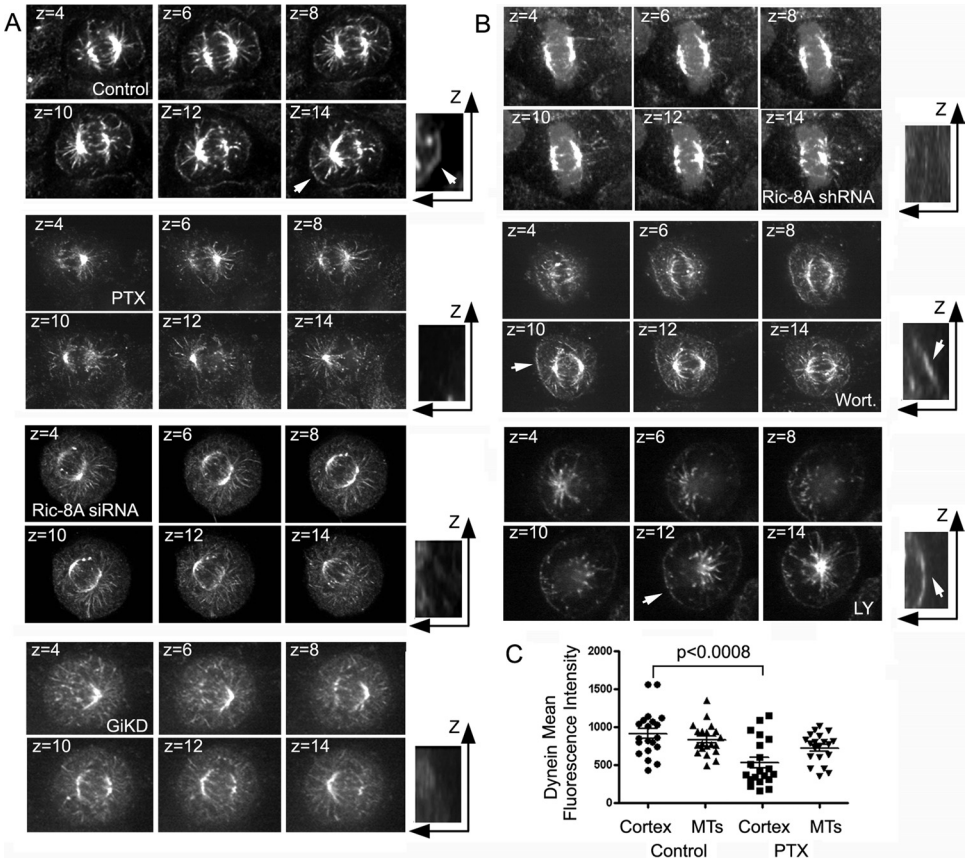

FIG. 4. Accumulation of dynein at the metaphase cell cortex depends upon Ric-8A. (A) Cortical dynein localization in pertussis toxin, Ric-8 siRNA-treated, and $G\alpha_{i1\text{-}3}$ siRNA-treated cells. Shown are selected images from sequentially numbered z-stacks of images acquired from control, pertussis toxin (PTX, 400 ng/ml for 4 h), Ric-8A siRNAs, or $G\alpha_i$ siRNAs (GiKD). The indicated HeLa cells growing on collagen coated dishes, fixed, immunostained, and imaged (0.5 μm between slices). *x-z* projections of a portion of the cell are shown to the right (electronically zoomed ×2). An arrow in last panel of the control cells points to dynein at the cell cortex. (B) Distribution of cortical dynein in Ric-8A shRNA-treated cells or with reduced PI3K activity. Shown are selected images from sequentially numbered z-stacks of images acquired from Ric-8A shRNA-treated, wortmannin-treated (10 nM for 2 h), or LY294002-treated (100 μM for 2 h) HeLa cells. The cells were plated on collagen coated dished, fixed, immunostained, and imaged (0.5 μm between slices). *x-z* projections of a portion of the cell are shown to the right (electronically zoomed ×2). Arrows point to cortical dynein in the wortmannin- and LY294002-treated cells. (C) Levels of dynein at the cell cortex and associated with astral microtubules in control and pertussis toxin-treated cells. The distribution and the average (bar; means ± the SD; $n = 50$) fluorescence levels from the control and pertussis toxin-treated (PTX) cells are shown from along cell cortex or microtubules (MTs). Each value is the mean of three separate determinations along the cell cortex or from three microtubules. The *P* value was < 0.0008 compared to control as determined by the Mann-Whitney test.

relative to the substratum were determined. Images from confocal z-stack acquired at 0.5-μm intervals, and a *x-z* projection for each condition is shown (Fig. 3C). We measured the average angle of the mitotic spindles from control metaphase cells (7.3 to 12.4°), Ric-8A siRNA-treated cells (22.3°; SD = 15.8), Ric-8A shRNA-treated cells (38.9°; SD = 19), $G\alpha_i$ knockdown cells (25.7°; SD = 8.5), and wortmannin-treated cells (15.7°; SD = 15.1) (Fig. 3D). These data indicate that PI3K, $G\alpha_i$, and Ric-8A all contribute to orienting mitotic spindles relative to the substratum.

Reduced Ric-8A expression, pertussis toxin treatment, or reduced $G\alpha_i$ expression affects the localization of dynein, LGN, and NuMA at the metaphase cell cortex in HeLa cells. Dynein-dynactin motor complexes function in mitotic spindle positioning in budding yeasts, *C. elegans*, and mammalian cells (4, 19, 21, 34, 39). To test whether Ric-8A signaling affected the localization of dynein/dynactin motor complexes during metaphase, we first examined the localization of dynein in metaphase HeLa cells. We found dynein enriched at the cell cortex opposite the spindle poles and along microtubules. Rather than a uniform appearance along the cell cortex, dynein had a nonhomogenous distribution (see Movie S3 in the supplemental material). Treatment of HeLa cells with pertussis toxin, reduced Ric-8A expression (siRNA pool), or reduced $G\alpha_{i\text{-}3}$ expression (siRNA pool) all decreased the amount of dynein at the cell cortex (Fig. 4A; also see Movies S4 to S6 in the supplemental material). Similarly, the Ric-8 shRNA also decreased dynein at the cell cortex (see Movie S7 in the supplemental material), whereas treatment with either wortmannin (see Movie S8 in the supplemental material) or LY294002 had no such effect (Fig. 4B). Experiments investigating the location of $p150^{glued}$, a component of the dynactin complex,

gave results similar to those that examined the distribution of dynein (data not shown). Quantification of the amount of dynein at the cell cortex versus the amount associated with astral microtubules of 50 metaphase cells indicated that pertussis toxin treatment reduced dynein at the cell cortex without significantly affecting the amount associated with astral microtubules (Fig. 4C).

Dynactin and Lis1 also regulate metaphase spindle orientation in *Drosophila* neuroblasts (28). Absence of either protein leads to reduced spindle pole rocking and impaired metaphase spindle alignment. $G\alpha_i$, Pins (LGN related), and Mud (NuMA related) are all enriched at the neuroblast apical cortex and required for proper metaphase spindle alignment. To test the role of Ric-8A in assembling a signaling complex to mediate mitotic spindle orientation in HeLa cells, we interfered with Ric-8A signaling and then examined the localization and expression of $G\alpha_{i1}$, LGN, and NuMA. We had previously screened several $G\alpha_i$ antibodies, as well as different fixation approaches, before settling on three antibodies specific for $G\alpha_{i1}$, $G\alpha_{i2}$, and $G\alpha_{i3}$, respectively, and paraformaldehyde fixation, which best preserved the cortical staining of $G\alpha_i$. In metaphase cells, $G\alpha_{i1}$ had a crescentic distribution, enriched at the cell cortex adjacent to the spindle poles, while at prophase it colocalized with actin enriched substrate attachment sites (see Fig. S1 in the supplemental material). Similar to dynein, it varied along the metaphase cell cortex. The distribution of $G\alpha_{i1}$ and NuMA at the cell cortex closely approximated each other at metaphase (Fig. 5A and B). In *Drosophila* neuroblasts increasing $G\alpha_i$ levels facilitate $G\alpha_i$ binding to the GoLoco 2 and 3 sites in Pins, which frees the tetratricopeptide repeats (TPRs) in Pins to recruit Mud to the apical cortex (22). Treating HeLa cells with pertussis toxin or reducing Ric-8A expression decreased the amount of $G\alpha_{i1}$ at the cell cortex adjacent to the spindle poles and, likely as a consequence, LGN and NuMA failed to accumulate (Fig. 5A). Quantification of the amount of $G\alpha_{i1}$ and NuMA along the cell cortex confirmed their reductions (Fig. 5C and D). In contrast, wortmannin treatment did not reduce $G\alpha_{i1}$ expression at the cell cortex nor that of LGN and NuMA (Fig. 5A). To verify that the wortmannin reduced PI3K activity, we imaged metaphase HeLa cells immunostained for phosphorylated AKT (pAKT). Consistent with the metaphase cell cortex localization of AKT-PH-GFP (34), we found that pAKT present at the cell cortex adjacent to the spindle poles, but in addition we detected pAKT in centrosomes and at the centromere region. Treatment with wortmannin reduced the amount at the cell cortex without obviously affecting the centrosome localization. Pertussis toxin treatment, Ric-8A knockdown, and $G\alpha_i$ knockdown also reduced the levels of pAKT at the cell cortex (Fig. 5A).

The accumulation of NuMA and LGN at the HeLa cell cortex adjacent to the spindle poles depends on normal microtubule function. As previously mentioned in *Drosophila* neuroblasts the asymmetric localization of Pins/$G\alpha_i$ is mediated by two partially redundant pathways. In one, Cdc42 colocalizes with Par-6, Inscuteable, and an atypical protein kinase C asymmetrically at the apical cortex of embryonic neuroblasts to induce Pins/$G\alpha_i$ cortical polarity (29). However, in mitotic HeLa cells these proteins localized homogenously at the cell cortex (data not shown). In the other pathway, microtubules, Khc-73, and Dlg function to coordinate neuroblast cortical polarity with the mitotic spindle (27). To test the role of microtubules in the localization of $G\alpha_{i1}$/LGN/NuMA, we treated HeLa cells with nocodazole. Nocodazole treatment disrupted microtubules and markedly inhibited the crescentic localization of these proteins although some $G\alpha_{i1}$ and LGN appeared along the mitotic cell cortex. In addition, some $G\alpha_{i1}$ accumulated in the cytosol. A lower concentration of nocodazole, sufficient to disrupt astral microtubules without grossly affecting spindle microtubules, also inhibited the cortical distribution of NuMA and LGN. In contrast, nocodazole treatment did not affect Ric-8A localization (Fig. 5E, first three panels). Taxol is a microtubule-stabilizing drug that induces the formation of microtubule asters in the cytoplasm of mitotic cells. Treatment of HeLa cells with Taxol also did not affect the localization of Ric-8A, but it did cause a loss of the crescentic localization of LGN, NuMA, and $G\alpha_{i1}$ (Fig. 5E, last three panels). Again, some $G\alpha_{i1}$ accumulated in the cytosol of the Taxol-treated cells. Thus, the accumulation of NuMA and LGN at the spindle pole cell cortex during the HeLa cell mitosis depends not only upon the presence of $G\alpha_i$, Ric-8A, and $G\alpha_i$ nucleotide exchange but also on normal microtubule function.

Imaging α-tubulin-GFP in Ric-8A knockdown cells reveals defects in mitosis and mitotic spindle movement. To provide further insights into the consequences of reducing Ric-8A function, we introduced control or Ric-8A siRNAs into HeLa cells constitutively expressing a α-tubulin-GFP fusion protein (HeLa-tubulin-GFP) and performed overnight live cell imaging, collecting a four-image z-stack every 3 min (see Movies S9 to S12 in the supplemental material). Reducing Ric-8A expression using either the siRNA pool or using the Ric-8A shRNA decreased the mitotic frequency and increased the percentage of mitotic failures. Some cells remained arrested for prolonged periods of time (Fig. 6A). Measuring the length of mitosis in control HeLa cells and in similar cells treated with the Ric-8A siRNA pool revealed an ca. 70% increase in the average duration of mitosis in the knockdown cells (Fig. 6B). To determine whether the loss of Ric-8A affected mitotic spindle movement, we imaged HeLa-tubulin-GFP cells treated with a siRNA control and similar cells treated with the Ric-8A siRNA pool. Shown are terminal images from time-lapse series spanning the duration of mitosis of five control and five knockdown cells (Fig. 6C). The orientation of the spindle axis was determined (every 3 min) and then sequentially overlaid over the final images. From this analysis the relatively stable mitotic spindle orientation and greater duration of mitosis observed with the Ric-8A knockdown cells is evident. Finally, we collected a time series of images from metaphase cells in either control siRNA-treated or Ric-8A siRNA-treated cultures. In these experiments we acquired the images every 30 s for 10 min and traced the movements of the spindle pole of control siRNA and Ric-8A siRNA-treated cells over that duration. This analysis also revealed reduced spindle pole movement in the knockdown cells (Fig. 6D, see Movies S13 and S14 in the supplemental material). The decreased mitotic spindle movement after reduction of Ric-8A expression is in contrast to the observed enhancement in spindle movements that followed overexpression of LGN or $G\alpha_i$ (3, 9).

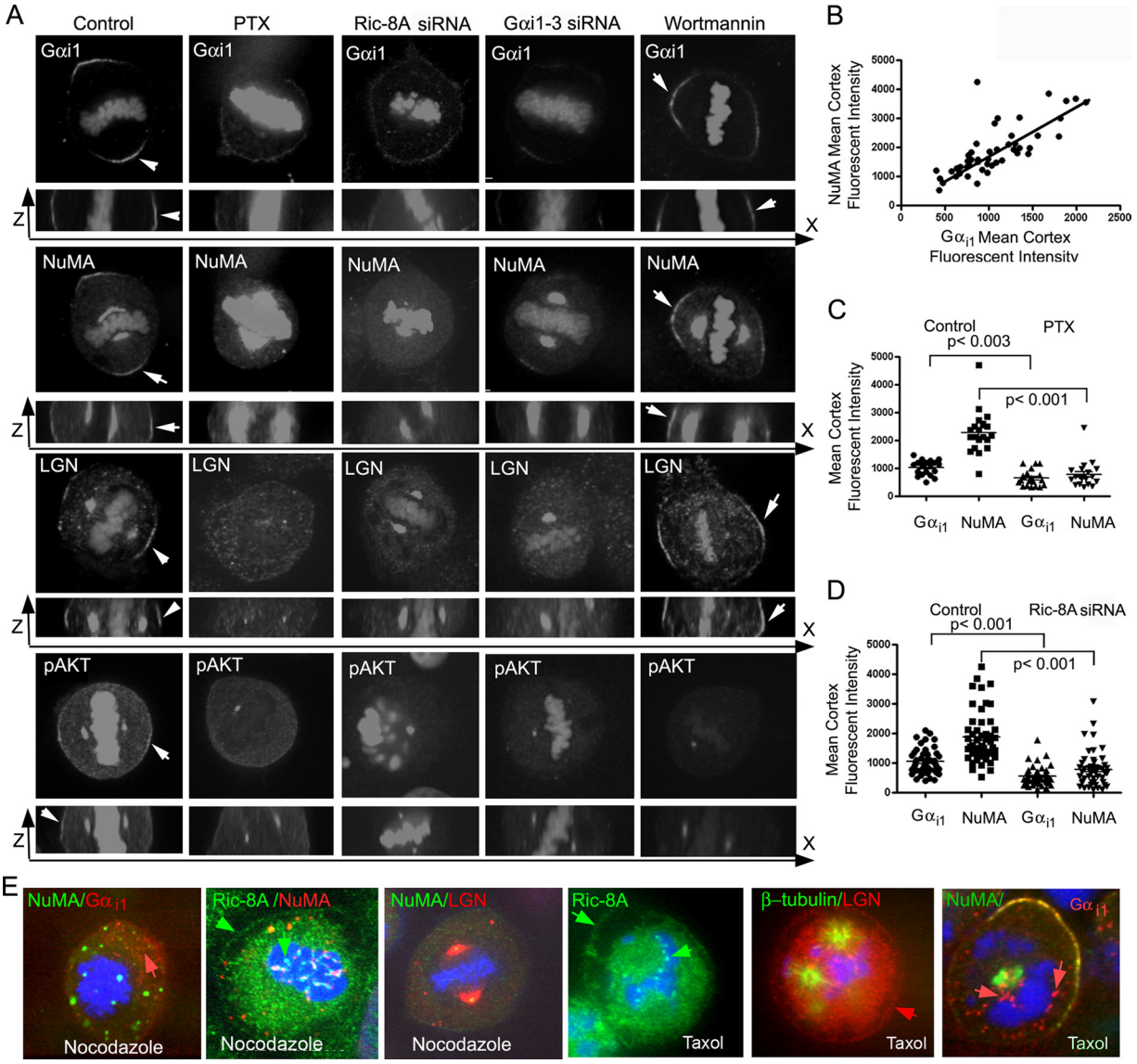

FIG. 5. The accumulation of $G\alpha_{i1}$, NuMA, LGN, and pAKT at the metaphase cell cortex depends upon Ric-8A and intact microtubules. (A) Effect of pertussis toxin, Ric-8A siRNAs, $G\alpha_i$ siRNAs, and wortmannin on $G\alpha_{i1}$, NuMA, LGN, and pAKT localization along the metaphase cell cortex. Shown are selected images from sequentially numbered z-stacks, which were acquired from control and pertussis toxin-, Ric-8A siRNA-, $G\alpha_i$ siRNA-, or wortmannin-treated HeLa cells plated on collagen coated dishes (0.5 μm between slices). *x-z* projections are shown underneath. (B) Correlation between $G\alpha_{i1}$ and NuMA present at the metaphase cell cortex. Each value is the mean of three determinations along the cell cortex opposite the spindle pole ($R^2 = 0.57$; P [two-tailed] < 0.0001). (C) Localization of $G\alpha_{i1}$ and NuMA at the metaphase cortex following pertussis toxin treatment. The distribution and averages (bar; means ± the SD; $n = 20$) of fluorescence levels from control and pertussis toxin-treated (PTX) cells of $G\alpha_{i1}$ and NuMA on the cell cortex (unpaired t test for the first versus the third column and the second versus the fourth column) are indicated. (D) $G\alpha_{i1}$ and NuMA on the metaphase cell cortex of Ric-8A knockdown cells. The distribution and averages (bar; means ± the SD; $n = 50$) of fluorescence levels of $G\alpha_{i1}$ and NuMA on the metaphase cell cortex from control and Ric-8A knockdown cells (unpaired t test for the first versus the third column and the second versus the fourth column) are indicated. (E) Effect of nocodazole and Taxol on LGN, NuMA, $G\alpha_{i1}$, and Ric-8A. HeLa cells were treated with nocodazole (500 or 100 nM, low) for 2 h or with Taxol (200 nM) and then immunostained as indicated. Individual panels show representative mitotically arrested cells. The lower concentration of nocodazole (third panel) did not disrupt the mitotic spindle but did impair astral microtubules. Red arrows in first and last panels indicate cytosolic $G\alpha_{i1}$. The red arrow in second to last panel indicates LGN at the cell cortex, while Ric-8A localization is indicated by green arrows in the second and fourth panels.

DISCUSSION

This study demonstrates that in adherent mammalian cells Ric-8A functions to assemble signaling complexes on the metaphase cell cortex, and it is crucial for appropriately orienting the spindle poles in response to cortical cues. In prophase and metaphase the Ric-8A antibody localized Ric-8A at the spindle poles, uniformly along the cell cortex, in the cytosol, and in a centromerelike pattern on chromosomes. ADP-ribosylation of $G\alpha_i$ subunits with pertussis toxin blocked Ric-8A-triggered nucleotide exchange. Treating cells with pertussis toxin, reducing Ric-8A expression, or decreasing $G\alpha_i$ expression all had a similar effect; they interfered with the normal orientation of

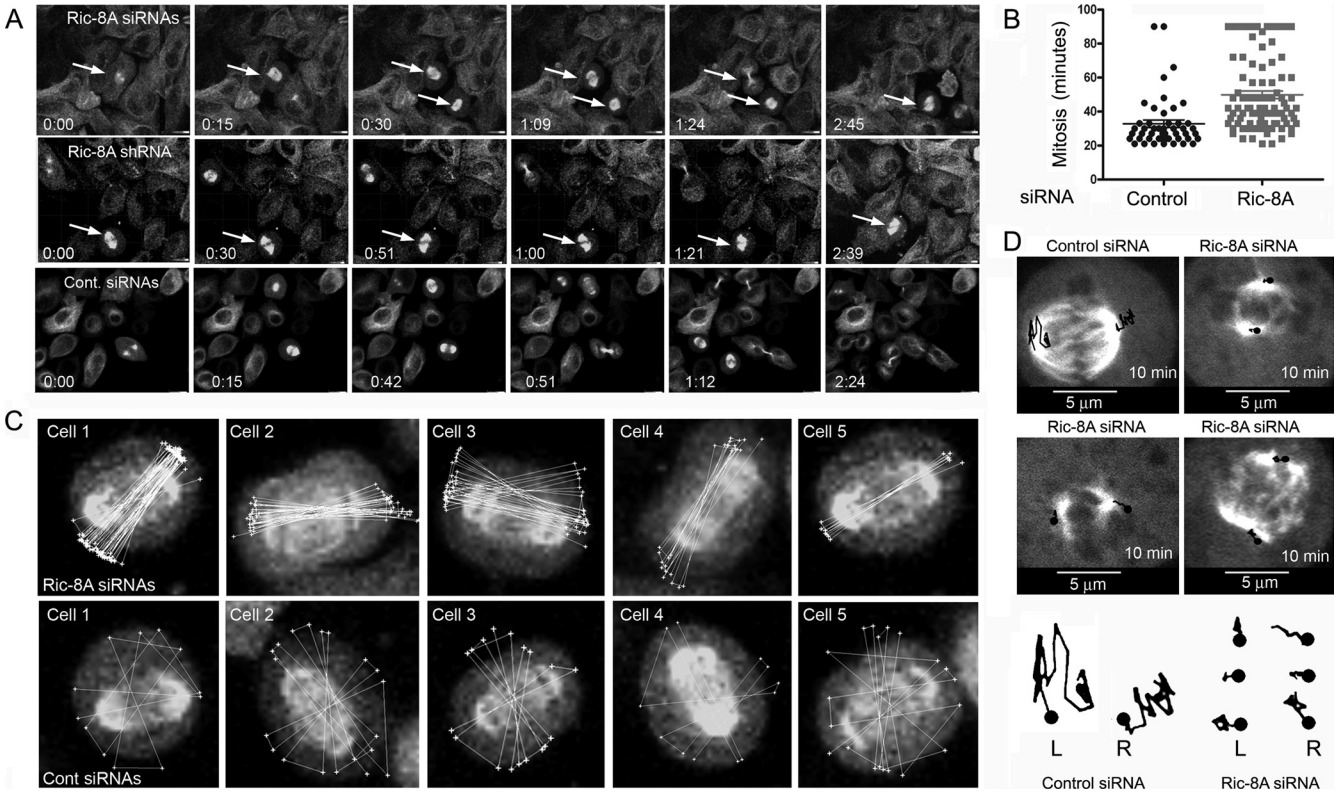

FIG. 6. Ric-8A knockdown causes prolonged mitoses, occasional mitotic arrest, and reduced mitotic spindle movement. (A) Maximum projection images from live cell imaging of Ric-8A knockdown (siRNA [top] or shRNA [middle]) or control (bottom) α-tubulin-GFP HeLa cells. Individual images (times are indicated in "hours:minutes" in each panel) were selected. Arrows indicate mitotic cells of note. (B) Duration of mitoses and cytokinesis in control and Ric-8A knockdown. The amount of time required from formation of the mitotic spindle to spindle separation was measured using recordings from live cell imaging experiments. For control cells the durations of 76 mitoses were measured, while for Ric-8A siRNA-treated cells 121 mitoses were measured. (C) Decreased spindle motion in Ric-8 knockdown cells. Maximum projection images from five cells treated with the Ric-8A siRNA pool (top) or five control HeLa-tubulin-GFP cells (expressing a control siRNA, bottom). Three days after transfection, mitotic cells were imaged every 3 min. The polygon function in Imaris was used to trace the mitotic spindle axis in relation to the cell body beginning with the second image acquired during mitosis. Overlaid white lines that cross the cell center indicate the spindle axis orientation, while the spindle rotation is indicated by white connecting lines at the cell periphery. (D) Spindle pole movements of a control cell or three siRNA Ric-8A treated cells. The cells were imaged for 10 min at 30-s intervals, and the location of each of the spindle poles was traced (shown in black lines) on the image and transposed below.

mitotic spindles to the substratum. Pertussis toxin treatment of MDCK cells also inhibited their normal mitotic spindle orientation. In contrast to the substratum, cell-cell contacts predominantly provide cortical cues used by MDCK cells for spindle alignment (24). Mammalian cells dividing on a substrate accumulated $G\alpha_i$, LGN, NuMA, and dynein along the cell cortex adjacent to the spindle poles during metaphase. Treatment with pertussis toxin or reduction of Ric-8A expression inhibited the enrichment of $G\alpha_i$ at these sites and LGN, NuMA, the $p150^{glued}$ component of dynactin, and dynein intermediate chain failed to accumulate. Long-term imaging of GFP-tubulin expressing cells with reduced Ric-8A levels revealed that these cells had prolonged mitoses and had reduced mitotic spindle movements compared to control cells.

The treatment of HeLa cells with pertussis toxin or the reduction of either $G\alpha_i$ or Ric-8A expression reduced the accumulation of the dynein/dynactin complex at the cell cortex, thereby providing a mechanism for the failure of the cells to appropriately align their mitotic spindles to the substratum. In yeast dynein is off-loaded from the microtubule plus end to Num1 sites present at the cell cortex (16). Subsequently, cortically anchored dynein powers the sliding of astral microtubules, which pulls the mitotic spindle toward the anchored sites (16). Since NuMA has been previously shown to form a complex with dynein and dynactin (17), it may serve a similar role as Num1 functioning to capture dynein/dynactin complexes at the cell cortex. NuMA can also provide a physical link between dynein/dynactin and the G-protein regulators LGN/AGS-3. The inability of LGN to accumulate on the metaphase cell cortex following Ric-8A or $G\alpha_i$ knockdown likely explains the reduction in NuMA there and, as a consequence, the appearance of the dynein/dynactin complexes. LGN provides a physical linkage between NuMA and $G\alpha_i$-GDP. In mammalian cell, overexpression of $G\alpha_i$-GDP can recruit LGN to the cell cortex (3, 9). Thus, the failure to enrich $G\alpha_i$ at the cell cortex opposite the spindle poles in the pertussis toxin-treated or in the Ric-8A knockdown cells likely explains the failure of LGN and NuMA to accumulate.

The analysis of asymmetric cell divisions in *Drosophila* and *C. elegans* has arrived at several different models of receptor-

independent heterotrimeric G-protein function (1, 2, 5, 8, 11, 36, 37). A consensus exists that one of the functions of Ric-8 is to target $G\alpha_i$ and $G\beta$ to the cell cortex during early development (2, 8, 11, 16). In its absence *Drosophila* $G\alpha_i$ and $G\beta$13F failed to appear on the neuroblast cell cortex and in *C. elegans* the $G\alpha$ subunit GPA-16 did not appear at the cell cortex although another $G\alpha$ subunit, GOA-1 did (2, 8, 11, 16). Ric-8 bound GPA-16 but did not trigger nucleotide exchange *in vitro*, arguing that GPA-16 cortical targeting did not require Ric-8 GEF activity (2). In model organisms the target of Ric-8 GEF activity is unclear. Some evidence suggests that Ric-8 acts on the heterotrimer to release $G\alpha_i$-GTP, which upon conversion to $G\alpha_i$-GDP binds a guanine dissociation inhibitor (GDI) such as GPR-1/2 or PINS. Other evidence suggests that Ric-8 acts on $G\alpha_i$-GDP/GDI to release $G\alpha_i$-GTP and the GDI. The active signaling molecule(s) in the various models also differ as roles for $G\beta\gamma$, $G\alpha_i$-GTP, and $G\alpha_i$-GDP/GDI have been ascribed (1, 2, 8, 11, 16). Consistent with some of the data in model organisms, the analysis of asymmetric cell division in the mouse cerebral cortex suggested that Ags3 (another Pins homologue related to LGN) triggers the release of $G\beta\gamma$ from $G\alpha_{i3}$. Silencing Ags3 gave a similar phenotype as impairing $G\beta\gamma$ signaling. Interference with $G\beta\gamma$ function caused a shift in the mitotic spindle orientation from apical-basal to planar (26). Although the role of Ric-8A was not addressed here, it would be predicted to act downstream of the AGS3-$G\alpha_i$-GDP complex to release AGS3 from $G\alpha_i$. As mentioned in the introduction, biochemical studies using mammalian proteins have provided some insights into the likely function of noncanonical G-protein signaling in mammalian cells (30, 31, 33). Ric-8A has GEF activity for several $G\alpha$ subunits but not as heterotrimers. Ric-8A preferentially acts on $G\alpha_i$-GDP bound to a GDI such as LGN or AGS3 releasing $G\alpha_i$-GTP and the GDI. LGN bound to $G\alpha_i$-GDP can recruit NuMA and thereby prevents its association with microtubules. *In vitro*, Ric-8A can release NuMA from LGN through control of allosteric $G\alpha_i$-GDP binding.

Based on the biochemical observations with mammalian proteins, previous mammalian studies of $G\alpha_i$, LGN, and NuMA, and our own studies we favor the following model to explain their role in mitotic spindle alignment. After breakdown of the nuclear membrane NuMA is released, allowing it to associate with cytosolic LGN, thereby increasing the affinity of LGN for $G\alpha_i$-GDP. Since almost all $G\alpha$ in HeLa cells is associated with $G\beta\gamma$ (14), LGN/NuMA can either target the heterotrimer displacing $G\beta\gamma$ and/or associate with newly synthesized $G\alpha_i$. Any freed $G\beta\gamma$ will likely activate downstream effectors. This may provide a mechanism for the activation of small GTPases and PI3K. Cortical Ric-8A GEF activity releases NuMA, LGN, and $G\alpha_i$-GTP. NuMA likely binds a cortical attachment factor to anchor it at the cell cortex. Freed of LGN, NuMA can interact with dynein/dynactin/Lis1-loaded microtubules to generate pulling forces. RGS proteins at the cell cortex accelerate the conversion of $G\alpha_i$-GTP to $G\alpha_i$-GDP, which can recruit additional NuMA/LGN, as well as reassociate with $G\beta\gamma$ to form the heterotrimer. Astral microtubules likely have some role in providing signals or even in delivering LGN, NuMA, and $G\alpha_i$ to the cell cortex adjacent to the spindle poles since their disruption with nocodazole decreased the crescentic appearance of all three proteins without impacting the cortical localization of Ric-8A.

A critical question is how Ric-8A acts to enrich $G\alpha_{i1}$ at the cell cortex adjacent to the spindle poles in metaphase HeLa cells? Heterotrimeric G proteins traffic to the cell cortex following their assembly in the cytosol and the myristoylation of $G\alpha$ and $G\gamma$. Insufficient $G\alpha$ production causes $G\beta\gamma$-subunit retention in the endoplasmic reticulum and, conversely, insufficient $G\beta$ subunit production dramatically reduces $G\alpha$ levels. Since immunostaining $G\beta_1$ and $G\beta_2$ in HeLa cells revealed no apparent change in their distribution in metaphase cells (H. Cho, unpublished observation), the increased $G\alpha_{i1}$ at the cell cortex opposite the spindle pole is likely associated with LGN/NuMA, not $G\beta\gamma$. The reduction of $G\alpha_{i1}$ at the HeLa metaphase cell cortex following pertussis toxin treatment argues that a direct binding of Ric-8A to $G\alpha_{i1}$ is needed for the accumulation. Ric-8A itself does not accumulate in a crescentic fashion at the cell cortex, arguing that it does not act as a localization factor for $G\alpha_i$. However, enhanced Ric-8A activity at the cell cortex opposite the spindle poles could provide a mechanism for the accumulation of $G\alpha_i$. Another possibility is that Ric-8A also acts in the cytosol to promote $G\alpha_i$ localization, perhaps by functioning as a chaperone. Astral microtubules that interact with the cell cortex may either deliver a signal or provide a direct delivery route for $G\alpha_i$ via microtubule-based transport (15). $G\alpha_i$-GTP is known to bind microtubules while $G\alpha_i$-GDP does not (7). In *Drosophila* it has been proposed that Ric-8 might promote the lipid modification of $G\alpha_i$ or even negatively regulate the removal of $G\alpha_i$ from the cell cortex (36); however, in HeLa cells these mechanisms seem unlikely.

In conclusion, our data indicate that Ric-8A is a key regulator of the dynamic localization, spatial interactions, and functions of a $G\alpha_i$/LGN/NuMA complex in mammalian cell division. The accumulation of this complex along the cell cortex adjacent to the spindle poles of metaphase cells depends upon Ric-8A. Ongoing $G\alpha_i$ nucleotide exchange likely causes the liberation of NuMA at these sites where it may function to capture dynein/dynactin complexes. This would facilitate the off-loading of dynein/dynactin complexes from astral microtubules to generate the pulling forces needed to center the spindle poles. Depression of Ric-8A or pertussis toxin treatment impairs $G\alpha_i$ nucleotide exchange, thereby inhibiting the release of $G\alpha_i$-GTP and NuMA from $G\alpha_i$-GDP/LGN/NuMA complexes. The disoriented mitotic spindles, reduced spindle pole movements, and the halting of mitosis result from disturbances in the dynamic interactions between LGN, $G\alpha_i$, and NuMA. In addition, studies using pertussis toxin need to consider that the ADP-ribosylation of $G\alpha_i$ affects not only GPCR GEF activity but also that of Ric-8A.

ACKNOWLEDGMENTS

We thank M. Rust for excellent editorial help, J. Blumer for the LGN antibody, and A. Fauci for continued support.

This research was supported by the intramural program of the National Institutes of Allergy and Infectious Diseases.

REFERENCES

1. **Afshar, K., F. S. Willard, K. Colombo, C. A. Johnston, C. R. McCudden, D. P. Siderovski, and P. Gonczy.** 2004. RIC-8 is required for GPR-1/2-dependent Gα function during asymmetric division of *Caenorhabditis elegans* embryos. Cell **119:**219–230.

2. **Afshar, K., F. S. Willard, K. Colombo, D. P. Siderovski, and P. Gonczy.** 2005. Cortical localization of the Gα protein GPA-16 requires RIC-8 function during *Caenorhabditis elegans* asymmetric cell division. Development **132:** 4449–4459.
3. **Blumer, J. B., R. Kuriyama, T. W. Gettys, and S. M. Lanier.** 2006. The G-protein regulatory (GPR) motif-containing Leu-Gly-Asn-enriched protein (LGN) and Giα3 influence cortical positioning of the mitotic spindle poles at metaphase in symmetrically dividing mammalian cells. Eur. J. Cell Biol. **85:**1233–1240.
4. **Busson, S., D. Dujardin, A. Moreau, J. Dompierre, and J. R. De Mey.** 1998. Dynein and dynactin are localized to astral microtubules and at cortical sites in mitotic epithelial cells. Curr. Biol. **8:**541–544.
5. **Couwenbergs, C., A. C. Spilker, and M. Gotta.** 2004. Control of embryonic spindle positioning and Gα activity by *Caenorhabditis elegans* RIC-8. Curr. Biol. **14:**1871–1876.
6. **Crouch, M. F., G. W. Osborne, and F. S. Willard.** 2000. The GTP-binding protein $G_{i\alpha}$ translocates to kinetochores and regulates the M-G_1 cell cycle transition of Swiss 3T3 cells. Cell Signal. **12:**153–163.
7. **Dave, R. H., W. Saengsawang, J. Z. Yu, R. Donati, and M. M. Rasenick.** 2009. Heterotrimeric G-proteins interact directly with cytoskeletal components to modify microtubule-dependent cellular processes. Neurosignals **17:** 100–108.
8. **David, N. B., C. A. Martin, M. Segalen, F. Rosenfeld, F. Schweisguth, and Y. Bellaiche.** 2005. Drosophila Ric-8 regulates Gαi cortical localization to promote Gαi-dependent planar orientation of the mitotic spindle during asymmetric cell division. Nat. Cell Biol. **7:**1083–1090.
9. **Du, Q., and I. G. Macara.** 2004. Mammalian Pins is a conformational switch that links NuMA to heterotrimeric G proteins. Cell **119:**503–516.
10. **Du, Q., P. T. Stukenberg, and I. G. Macara.** 2001. A mammalian Partner of inscuteable binds NuMA and regulates mitotic spindle organization. Nat. Cell Biol. **3:**1069–1075.
11. **Hampoelz, B., O. Hoeller, S. K. Bowman, D. Dunican, and J. A. Knoblich.** 2005. *Drosophila* Ric-8 is essential for plasma-membrane localization of heterotrimeric G proteins. Nat. Cell Biol. **7:**1099–1105.
12. **Hepler, J. R., and A. G. Gilman.** 1992. G proteins. Trends Biochem. Sci. **17:**383–387.
13. **Kaji, N., A. Muramoto, and K. Mizuno.** 2008. LIM kinase-mediated cofilin phosphorylation during mitosis is required for precise spindle positioning. J. Biol. Chem. **283:**4983–4992.
14. **Krumins, A. M., and A. G. Gilman.** 2006. Targeted knockdown of G protein subunits selectively prevents receptor-mediated modulation of effectors and reveals complex changes in non-targeted signaling proteins. J. Biol. Chem. **281:**10250–10262.
15. **Levy, J. R., and E. L. Holzbaur.** 2007. Special delivery: dynamic targeting via cortical capture of microtubules. Dev. Cell **12:**320–322.
16. **Markus, S. M., J. J. Punch, and W. L. Lee.** 2009. Motor- and tail-dependent targeting of dynein to microtubule plus ends and the cell cortex. Curr. Biol. **19:**196–205.
17. **Merdes, A., K. Ramyar, J. D. Vechio, and D. W. Cleveland.** 1996. A complex of NuMA and cytoplasmic dynein is essential for mitotic spindle assembly. Cell **87:**447–458.
18. **Mitsushima, M., F. Toyoshima, and E. Nishida.** 2009. Dual role of Cdc42 in spindle orientation control of adherent cells. Mol. Cell. Biol. **29:**2816–2827.
19. **Muhua, L., T. S. Karpova, and J. A. Cooper.** 1994. A yeast actin-related protein homologous to that in vertebrate dynactin complex is important for spindle orientation and nuclear migration. Cell **78:**669–679.
20. **Neer, E. J.** 1995. Heterotrimeric G proteins: organizers of transmembrane signals. Cell **80:**249–257.
21. **Nguyen-Ngoc, T., K. Afshar, and P. Gonczy.** 2007. Coupling of cortical dynein and G alpha proteins mediates spindle positioning in Caenorhabditis elegans. Nat. Cell Biol. **9:**1294–1302.
22. **Nipper, R. W., K. H. Siller, N. R. Smith, C. Q. Doe, and K. E. Prehoda.** 2007. Gαi generates multiple Pins activation states to link cortical polarity and spindle orientation in *Drosophila* neuroblasts. Proc. Natl. Acad. Sci. U. S. A. **104:**14306–14311.
23. **Pearson, C. G., and K. Bloom.** 2004. Dynamic microtubules lead the way for spindle positioning. Nat. Rev. Mol. Cell. Biol. **5:**481–492.
24. **Reinsch, S., and E. Karsenti.** 1994. Orientation of spindle axis and distribution of plasma membrane proteins during cell division in polarized MDCKII cells. J. Cell Biol. **126:**1509–1526.
25. **Ruchaud, S., M. Carmena, and W. C. Earnshaw.** 2007. Chromosomal passengers: conducting cell division. Nat. Rev. Mol. Cell. Biol. **8:**798–812.
26. **Sanada, K., and L. H. Tsai.** 2005. G protein βγ subunits and AGS3 control spindle orientation and asymmetric cell fate of cerebral cortical progenitors. Cell **122:**119–131.
27. **Siegrist, S. E., and C. Q. Doe.** 2005. Microtubule-induced Pins/Gαi cortical polarity in *Drosophila* neuroblasts. Cell **123:**1323–1335.
28. **Siller, K. H., and C. Q. Doe.** 2008. Lis1/dynactin regulates metaphase spindle orientation in *Drosophila* neuroblasts. Dev. Biol. **319:**1–9.
29. **Siller, K. H., and C. Q. Doe.** 2009. Spindle orientation during asymmetric cell division. Nat. Cell Biol. **11:**365–374.
30. **Tall, G. G., and A. G. Gilman.** 2005. Resistance to inhibitors of cholinesterase 8A catalyzes release of Gαi-GTP and nuclear mitotic apparatus protein (NuMA) from NuMA/LGN/Gαi-GDP complexes. Proc. Natl. Acad. Sci. U. S. A. **102:**16584–16589.
31. **Tall, G. G., A. M. Krumins, and A. G. Gilman.** 2003. Mammalian Ric-8A (synembryn) is a heterotrimeric Gα protein guanine nucleotide exchange factor. J. Biol. Chem. **278:**8356–8362.
32. **Thery, M., A. Jimenez-Dalmaroni, V. Racine, M. Bornens, and F. Julicher.** 2007. Experimental and theoretical study of mitotic spindle orientation. Nature **447:**493–496.
33. **Thomas, C. J., G. G. Tall, A. Adhikari, and S. R. Sprang.** 2008. Ric-8A catalyzes guanine nucleotide exchange on G α1 bound to the GPR/GoLoco exchange inhibitor AGS3. J. Biol. Chem. **283:**23150–23160.
34. **Toyoshima, F., S. Matsumura, H. Morimoto, M. Mitsushima, and E. Nishida.** 2007. PtdIns(3,4,5)P3 regulates spindle orientation in adherent cells. Dev. Cell **13:**796–811.
35. **Toyoshima, F., and E. Nishida.** 2007. Integrin-mediated adhesion orients the spindle parallel to the substratum in an EB1- and myosin X-dependent manner. EMBO J. **26:**1487–1498.
36. **Wang, H., K. H. Ng, H. Qian, D. P. Siderovski, W. Chia, and F. Yu.** 2005. Ric-8 controls *Drosophila* neural progenitor asymmetric division by regulating heterotrimeric G proteins. Nat. Cell Biol. **7:**1091–1098.
37. **Wilkie, T. M., and L. Kinch.** 2005. New roles for Gα and RGS proteins: communication continues despite pulling sisters apart. Curr. Biol. **15:**R843–R854.
38. **Yang, F., D. G. Camp II, M. A. Gritsenko, Q. Luo, R. T. Kelly, T. R. Clauss, W. R. Brinkley, R. D. Smith, and D. L. Stenoien.** 2007. Identification of a novel mitotic phosphorylation motif associated with protein localization to the mitotic apparatus. J. Cell Sci. **120:**4060–4070.
39. **Yingling, J., Y. H. Youn, D. Darling, K. Toyo-Oka, T. Pramparo, S. Hirotsune, and A. Wynshaw-Boris.** 2008. Neuroepithelial stem cell proliferation requires LIS1 for precise spindle orientation and symmetric division. Cell **132:**474–486.